An axial flux generator for wind turbine in autonomous low-power production

Faradji Boubakar[1]* 🆔, Ameur Aissa[2] 🆔

[1]*Faculty of science and technology, Department of Electrical Engineering, University Amin Al-Akkal Haj Moussa Akhamok Tamanghesset, Algeria.*
[2]*Faculty of technology, Department of Electrical Engineering, University Amar Télidji Laghouat, Ageria.*

*Corresponding author: boubakarluck @yahoo.fr

Abstract:

The main objectify of this article subject is the study and feasibility of micro wind turbine used for small farms, the electrical power generated from an axial flux permanent magnet generator when the power scale is in direct correlation with wind velocity. The proposed design shows more economic costs with accepted recovered power. The originality of this proposed generator is due to the flexibility and malleability of stator windings' various positions connection which allowed it to pass from the signal phase to multiphase generator. The mechanical coupling between the generator and wind turbine is a direct drive system without mechanical gear when the rotor is designed to excite the stator from hollow disc permanent magnets. However, the generator electromagnetic model study with finite element analyses is carried out in three dimensions thanks to Flux3D accuracy software. The simulation results assent to the forefront of a decision to proceed with primary experimental tests on the designed prototype.

1. Introduction

A contemporary model farm cannot be satisfied and relies on only one source of electrical energy to operate all its mechanisms, and in conjunction with the development achieved in the field of renewable energies; it can be resorted to as a solution to provide the necessary energy. To be able to take a position in the competitive renewable energy market light, wind turbines must present the lowest construction cost possible with the best performances of course.

The use of a direct drive system in wind turbines is not a new proposal and several studies offered to eliminate the gearbox from the drive chain, in [1] the mechanical faults caused by gearbox vibration perturb all control systems for the generator, even in [2–4] the impact is a catastrophe on the wind turbine noises level. Economically gearbox can cost a very high price in fabrication and maintenance; all these dark points are avoided in a direct drive system and only one relative shift arm is used for the turbine and generator rotor Fig. 1 the low-speed arm. The generator rotor will spine over at the same speed as the turbine and generally it

has a low speed [5] dependent directly on wind velocity, to increase the generator rotor speed ratio the rotor magnetic poles number must be increased, this solution can not only reduce the rotor speed but also create a startup launch problem in generator starting due to the rotor excessive heavy mass and inertia, if the generator operates on principal classic radial flux machines. Contrarily, this problem can be handled in better condition in case of machine operates on the axial flux. The axial flux permanent magnet generator
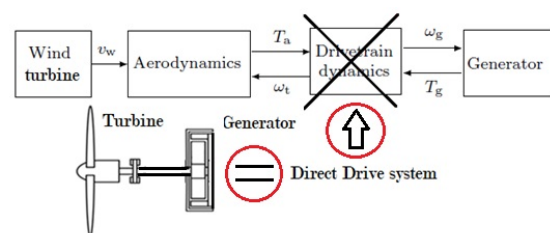

Figure 1. Total arrangement for wind turbine directed drive system with correspondent functionality blocks.

(AFPMG) can be designed in many different forms, in [6–10] a detailed comparison between classic radial, axial, and transversal permanent magnet machines is presented when advantages are clearly cited for each type. Based on this review, an estimation for a developed simple wind turbine prototype governs the old three-blade axial wind turbine and the new AFPMG in direct drive for small industrial prospects. In order to demonstrate the electromechanical performance of the proposed axial flux generator, a deep FEA in three dimensions views is applied to the generator model.

The specifications required to design an AFPMG intended for wind turbine power can be highlighted in [11–14]. From an industrial point of view, the new proposed prototype structure is more economical in terms of raw materials and process time than conventional wind turbines currently on this market. Afterward, this new AFPMG should promote the production of an alternative voltage in stator windings. From an electromagnetic point of view, the objectives are to obtain better specific power as well as better efficiency and voltage compared to conventional wind turbines developing the same useful power.

The work in this article is subdivided into three sections, in the first section, a theoretical review regarding the proposed AFPMG generator definition and design presentation is presented.

In the second section, AFPMG generator model is presented and FEM is used in the simulation of the generator in three dimensions.

In the last section, the AFPMG generator prototype is realized and test results are carried out under real conditions.

2. Presentation of system and AFPM generator operating principle

A cross-section for single side AFPMG generator is presented in Fig. 2, we can illustrate one pole stator and rotor detailed draw in Fig. 3. The generator stator windings are concentric coils in the form of the letter "O" and they occupied one side only of the stator. The stator itself is composed of two half-cylinders firmed from both sides, on the active side of the stator, 6 coils are directly fixed on a ferromagnetic disk, each two coil terminals are connected outside the stator, and the total number of coils is 6 coupled to create three phases generator. The composite material rotor is disk non-magnetic metal, when 6 ferrite permanent magnets are fixed up approximately in the same distances as stator coils
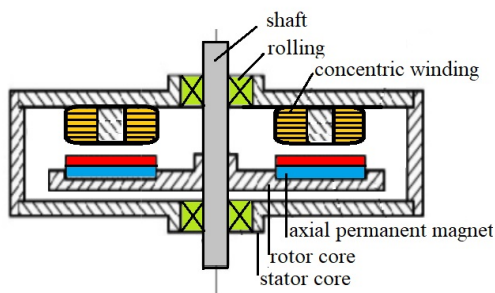
are fixed, the dimensions of stator coils are slightly different from magnets but in the same geometrical "O" form, and the magnets polarization sequence order is north than south (N,S,N,S,N,S) or the magnets are arranged on the rotor with their poles alternated. The rotor shaft is spinning around the two fixed rolling or bearings in the stator core armature, the magnetic field induced from each magnet will crossover the fixed stator concentric coil, and as a result a progressive alternate magnetic wave is created and the voltage is generated in the three phases, and the maximal value depends on rotor speed which is directly wind speed. Due to the low speed of the direct-driven generator, a large number of poles should be chosen, in order to get a frequency not too low, and consequently, a large number of stator coils are needed to construct the multi-pole windings.

Table 1 specifies the dimensions and ratings of the studied and fabricated prototype AFPMG three-phase generator.

3. Finite element 3D modeling and analysis for AFPMG generator

3.1 Model problem formulation

Axial flux generator being complex to model analytically [15], for that three-dimensional finite element analysis technique, provides accurate solutions in this case with similar precision required in axial flux machine performances analysis. The three-dimensional magnetic flux and field distributions in complex three-dimensional geometries and paths can be calculated with astonishing and sensitive resemblance to the real machine prototype faithfully. However, the 3DEFA technique requires a detailed definition of the geometry assumed to the initial design and boundary conditions equations must be solved too after magnetic problem formulation [16]. The design procedure here presented consists of a preliminary approach to the design methodology of AFPMG generator.

The magnetostatic problem model is obtained by neglecting the time derivatives in Maxwell equations [17].

$$
\begin{aligned}
\nabla \times \vec{H} &= \vec{J} & \nabla . \vec{J} &= 0 \\
\vec{B} &= \mu \vec{H} + \vec{B}_r & \nabla . \vec{B} &= 0 \\
\vec{B} &= \nabla \times \vec{A} & \nabla . \vec{A} &= 0
\end{aligned}
\tag{1}
$$

$\vec{J}$: current density
$\vec{H}$: magnetic field intensity
$\vec{B}$: magnetic flux density
$\vec{A}$: magnetic potential vector

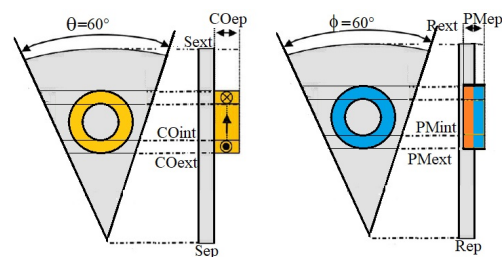**Figure 2.** A cross section for single side AFPMG generator.

Figure 3. AFPMG generator one pole stator and rotor detailed draw.

μ: magnetic permability

$\vec{B}_r$: magnetization vector of the PM

In this model, we assume that the magnetic field is produced by sources independent of time, and the electric fields $\vec{E}$ and magnetic $\vec{B}$ are decoupled, on the other hand, we wish to model an object traversed by non-zero currents. Thus, given a divergence-free stationary source current density $\vec{J}$, the relationships between the potential associated with the magnetic field are governed by the following equations:

$$\nabla \times (\frac{1}{\mu}\nabla \times \vec{A}) = \vec{J} + \nabla \times (\frac{1}{\mu}\vec{B}_r) \qquad (2)$$

The $\vec{J}$ represents the current density due to the current in the stator winding and the equivalent in the magnetizing current of the magnetization rotor magnets.

Solving equation specifying the boundary conditions of the domain study is carried out by the finite element method.

3.2 The AFPMG generator under FEA

To resolve electromagnetic problems with FEA, three steps must be respected, the geometry drawing, then geometry meshing, and finally exploitation of simulation results. The software Flux3D accuracy is a pioneer in this field of analysis.

The machine stator and the rotor geometry parameters material properties and coil type are directly defined in post-processor.

The AFPMG generator geometry in the Flux3D environment is depicted in Fig. 4, all parts under simulation, the airgap, the stator, the rotor, permanent magnets, and non-meshed coils are geometrically traced over and magnetically assigned according to Table 1.

Table 1. Design dimensions and specifications

Parameters	Description	Value	Unit
Stator			
Sext	The outer diameter of the stator	120	mm
Sep	Stator thiknis	5	mm
θ	Sator pole opning	60	degrees
E	Airgap	1	mm
L	Stator length	40	mm
Rotor			
Rext	Outer Rotor rayen	100	mm
Rep	Rotor thiknis	6	mm
ϕ	Rotor pole opning	60	mm
Coil			
COext	Coiles outer rayen	20	mm
COin	Inner diameter of Coile	10	mm
COep	Coiles thiknes	8	mm
N	Winding turns per coil	90	-
Wire	Coil Wire Section	0.63	mm^2
Coils	Coils number	6	-
Permanent magnet			
PMest	Magnet outer rayen	18	mm
PMint	Magnet inter rayen	10	mm
PMep	Magnet thicknes	6	mm
Magnets	Magnets number	6	-

The Fig. 5 illustrates AFPMG geometry mesh in Flux3D environment. Concerning the mesh choice this last must be fine enough to obtain precision correct but should not be too dense otherwise it will slow down strongly the calculations.

It was therefore decided that the stator yokes would be relatively coarsely meshed and the air gap much larger finely. In order to automate the mesh, a length of constant mesh throughout the machine equal to the value of the air gap is chosen. The meshes total elements number is 29213, with 5111 nodes.

3.3 Simulated and computed results in 3DFEA

Step by step in time in the no-load condition, the magnetic problem is resolved and the simulations results are recovered. Regarding the magnetic flux density distribution in the stator core, a detailed mapping is observed in Fig. 6 and Fig. 7 for a triangular cross-section, showing both stator sides and the stator of both two armatures, respectively. It is possible to see the local saturations of the magnetic circuit, the left side from the edge to the middle of stator but on the edge is greater than outer parts, the same observation on the right side too, the stator can be noted as symmetric with two magnetic poles.

As seen in Fig. 8 showing the visualization of the airgap flux density distribution, the flux-intensive distribution is located under the six magnets and stator coils in the air gap.
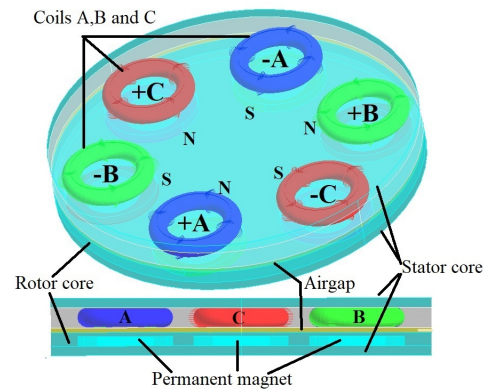

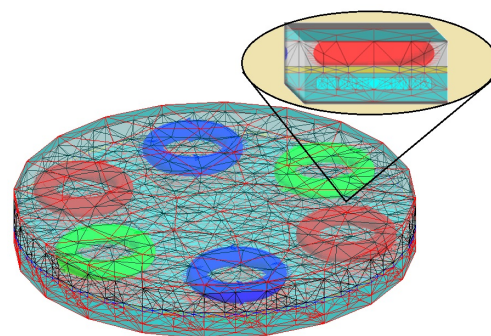**Figure 4.** The AFPMG generator geometry in Flux3D environment.

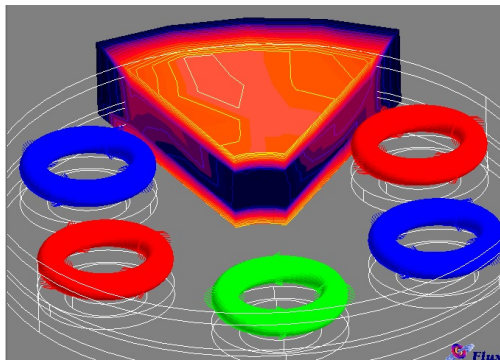**Figure 5.** The AFPMG generator geometry mesh in the Flux3D environment.

Figure 6. The Flux density distribution in the triangular cross-section shows both stator sides .
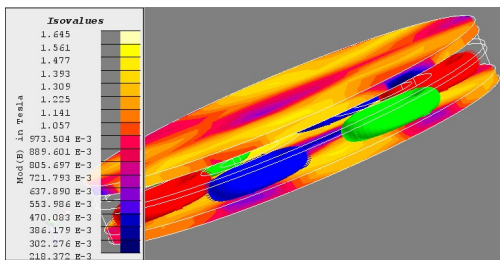

Figure 7. The AFPMG Flux density distribution on two stator sides.

Fig. 9 shows magnetic flux arrows density and path in all generators, the flux lines flow the permanent magnets polarization in Fig. 10. The stator coils are crossover directly by magnetic flux change polarization when the rotor is in rotation. The vector plot demonstrates the magnetization direction of the PM. They are axially magnetized.

4. AFPMG generator prototype and test results

AFPMG generator prototype has been physically developed and primer test results are carried out. The dimensioning of the generator is done iteratively via the numerical approach based on some simplifying assumptions and with the available technology in manufacturing at the laboratory. The design of the prototype was made under geometrical constraints imposed by the available ferromagnetic material.
Fig. 11 shows the generator prototype on the test bench. Supplementary elements are necessary before starting testes, which are the support post and the concrete footing to hold
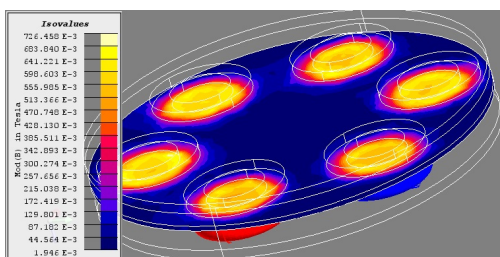

Figure 8. The AFPMG Flux density distribution in the air-gap.
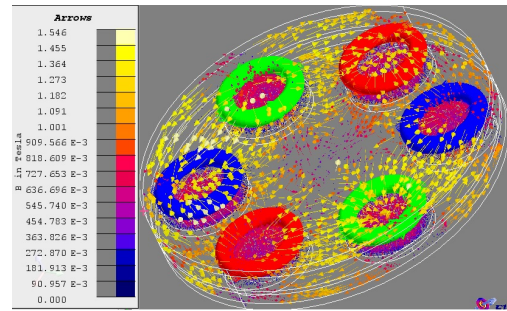

Figure 9. The AFPMG generator flux arrows density.

the wind turbine and allow the turbine free rotation.
The figure shows the rotor final view for permanent magnets arrangement in the generator rotor; and the stator coils positions with output wires terminals connections.
The AFPMG prototype tests cover the visualization of the induced voltage curve form and the calculation of voltage-induced value in each stator phase. The wind is supposed directly vertical on the turbine blades and it is generated by using an air blower, and wind speed is measured with a min-anemometer. For the visualization of voltage, a digital oscilloscope with two sondes is connected to each generator output terminal. Several tests are performed on the prototype generator under no-load conditions and the measured voltages have been registered in each case.
Fig. 12 and Fig. 13 illustrate the induced voltage for two different wind speeds in two separated coils in opposite positions for the same stator phase (-A and +A) , the depicted voltage is a sinusoidal shape curve in time for each coil. The induced voltages are in opposite variation too, test results demonstrate the registered results in FEM simulation, the voltage evaluation varies flowing the polarization of the magnets in the rotor. The maximum voltage value changes with the turbine's maximum rotation speed by comparing both figures. With a speed of 6 m/s, the voltage maximal value is around 2 V in coil.
To observe the phases voltages, the two coils are wired in series strings (start wire from one coil connects to the finish wire of the next in that phase, and so on), which are connected in a star (wye) configuration to form a three
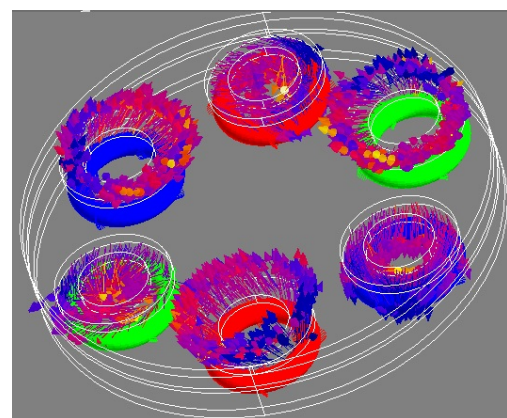

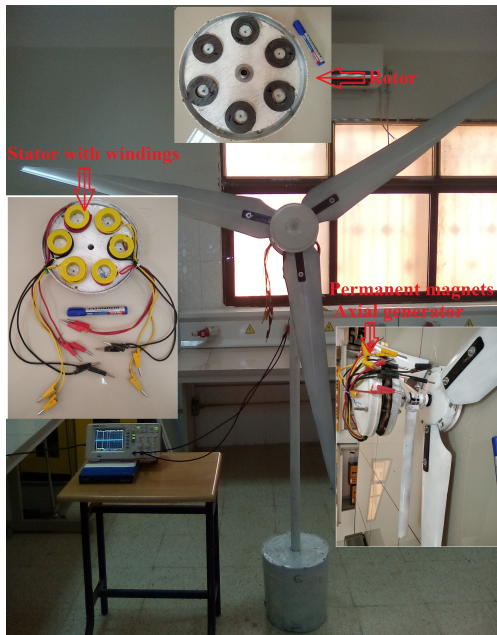**Figure 10.** The AFPMG generator permanent magnets flux arrows density.

Figure 11. The AFPMG prototype generator test bench, the rotor disk and stator.

Figure 12. Experimental results of two stator coils voltage at 6 m/s for (50 mV/div, 100 ms/div).

Figure 13. Experimental results of two stator coils voltage at 5.1 m/s for (50mV/div, 100ms/div).

phase generator, the evaluation of phase to neutral voltage is presented in Fig. 14, the wind turbine records a smell value around 3.1 m/s and the voltage curve is a sinusoidal presenting more picks and harmonics.

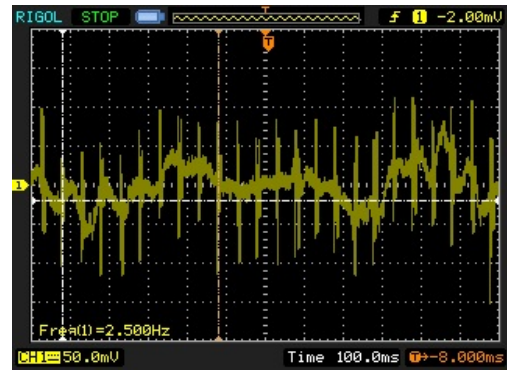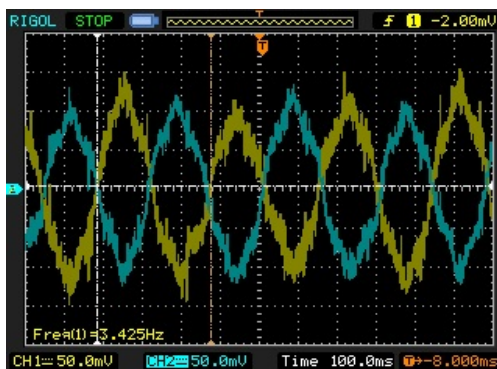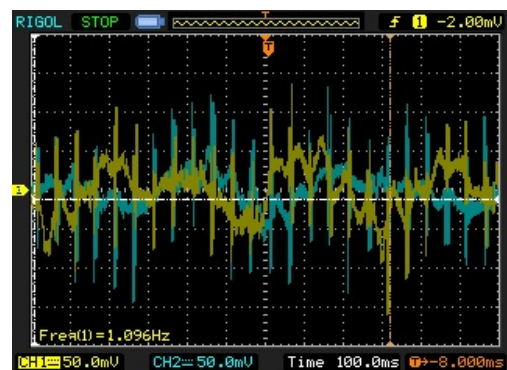The three phases are shifted one to other at 120° as it is pre-

Figure 14. Experimental results of one stator phase voltage at 3.1 m/s for (50 mV/div, 100 ms/div).

sented in Fig. 15 and Fig. 16. The voltage maximal value is 1 V at 3.1 m/s, with voltage picks of 2 V approximately, the increase of turbine speed increasing voltage value but voltage picks too.

Figure 15. Experimental results of two stator phases voltage A and B at 3.1 m/s for (50m V/div, 100 ms/div).

Figure 16. Experimental results of two stator phases voltage B and C at 3.1 m/s for (50 mV/div, 100 ms/div) .

5. Conclusion

Axial flux permanent speed direct drive generators actually present various possible structures, the proposed design is oriented to small-scale wind power applications. A simple electromagnetic design model, considering the fundamental laws governing this type of machine was used to achieve

and implement a prototype. This effort relies on a set of numerical models which lack the precision and accuracy that a final analysis deserves. Nevertheless, the obtained prototype accomplishes a good compromise between performance characteristics and feasibility of construction, validating further investigation and optimization of this machine structure is necessary in future works.

Authors Contributions
All the authors have participated sufficiently in the intellectual content, conception and design of this work or the analysis and interpretation of the data (when applicable), as well as the writing of the manuscript.

Availability of data and materials
Data presented in the manuscript are available via request.

Conflict of Interests
The authors declare that they have no known competing financial interests or personal relationships that could have appeared to influence the work reported in this paper.

Open Access
This article is licensed under a Creative Commons Attribution 4.0 International License, which permits use, sharing, adaptation, distribution and reproduction in any medium or format, as long as you give appropriate credit to the original author(s) and the source, provide a link to the Creative Commons license, and indicate if changes were made. The images or other third party material in this article are included in the article's Creative Commons license, unless indicated otherwise in a credit line to the material. If material is not included in the article's Creative Commons license and your intended use is not permitted by statutory regulation or exceeds the permitted use, you will need to obtain permission directly from the OICC Press publisher. To view a copy of this license, visit https://creativecommons.org/licenses/by/4.0.

References

[1] H. Gu, W. Y. Liu, Q. W. Gao, and Y. Zhang. "**A review on wind turbines gearbox fault diagnosis methods**.". *Journal Of Vibroengineering*, **23**(1):26–48, 2021. DOI: https://doi.org/10.21595/jve.2020.20178.

[2] B. Corley, J. Carroll, and A. Mc Donald. "**Fault detection of wind turbine gearbox using thermal network modelling and SCADA data**.". *Journal of Physics*, **1618**, 2020. DOI: https://doi.org/10.1088/1742-6596/1618/2/022042.

[3] Y. Pan, R. Hong, J. Chen, J. Fen, and W.Wu. "**Performance degradation assessment of wind turbine gearbox based on maximum mean discrepancy and multi-sensor transfer learning Structural**.". *Journal of Health Monitoring*, **20**(1):118–138, 2021. DOI: https://doi.org/10.1177/147592172091907.

[4] Y. Yang, A. Liu, H. Xin, and J. Wang. "**Fault early warning of wind turbine gearbox based on multi-input support vector regression and improved ant lion optimization**.". *Journal of Wind Energy*, **24**:812–832, 2021. DOI: https://doi.org/10.1002/we.2604.

[5] A. Bensalah, G. Barakat, and Y. Amara. "**Electrical generators for large wind turbine: trends and challenges**.". *Journal of MDPI Energies*, **15**(18):6700, 2022. DOI: https://doi.org/10.3390/en15186700.

[6] Y.Y. Ji and G.J. Li. "**Comparative study of axial-flux switched reluctance machine with different core materials**.". *2023 IEEE International Electric Machines & Drives Conf*, , 2022.

[7] G. Cakal and O. Keysan. "**Axial flux generator with novel flat wire for direct-drive wind turbines**.". *IET Renew Power Gener*, **15**:139–152, 2021. DOI: https://doi.org/10.1049/rpg2.12011.

[8] M. A. Yazdi, S. A. Saied, and S. M. Mirimani. "**Design and construction of new axial-flux permanent magnet motor**. ". *IET Electr. Power Appl*, **14**(12): 2389–2394, 2020. DOI: https://doi.org/10.1049/iet-epa.2020.0126.

[9] J. Du, P. Lu, and De. Liang. "**Optimal design of a linear transverse-flux machine with mutually coupled windings for force ripple reduction**. ". *IET Electr. Power Appl.*, **12**(2):271–280, 2018. DOI: https://doi.org/10.1049/iet-epa.2017.0227.

[10] A. Nyitrai and M. Kuczmann. "**Magnetic equivalent circuit and finite element modeling of anisotropic rotor axial flux permanent magnet synchronous motors with fractional slot distributed winding**.". *IET Electr. Power Appl.*, **17**(5):709–720, 2023. DOI: https://doi.org/10.1049/elp2.12298.

[11] K. Wirtayasa and C. Y. Hsiao. "**Performances comparison of axial-flux permanent magnet generators for small-scale vertical-axis wind turbine**.". *Alexandria Engineering Journal*, **61**:1201–1215, 2022. DOI: https://doi.org/10.1016/j.aej.2021.06.074.

[12] F. Kutt, K. Blecharz, and D. Karkosinski. "**Axial-flux permanent-magnet dual-rotor generator for a counter-rotating wind turbine**.". *Journal of MDPI Energies*, **13**(11):2833, 2020. DOI: https://doi.org/10.3390/en13112833.

[13] R. Toto, H. S. Sudarsono, and S. Muhammad. "**Performance of axial generator for a small vertical axis wind turbine**.". *Journal Européen des Systèmes Automatisés*, **56**(2):237–243, 2023. DOI: https://doi.org/10.18280/jesa.560208.

[14] S. A. Ashrafzadeh, A. A. Ghadimi, A. Jabbari, and M. R. Miveh. "**Optimal design of a modular axial-flux permanent-magnet synchronous generator for gearless wind turbine applications**.". *Journal of Wind Energy*, **27**(3):1–19, 2023. DOI: https://doi.org/10.1002/we.2887.

[15] R. Dorget and T. Lubin. "**Non-linear 3-D semi-analytical model for an axial flux reluctance mag- netic coupling**.". *IEEE Trans. En. Conv.*, **37**(3):2037–2047, 2022. DOI: https://doi.org/10.1109/TEC.2022.3153173.

[16] K. H. Kim and D. K. Woo. "**Novel quasi-three-dimensional modeling of axial flux in-wheel motor with permanent magnet skew**.". *IEEE Access*, **10**:98842 – 98854, 2017. DOI: https://doi.org/10.1109/ACCESS.2022.3206774.

[17] T. Okita and H. Harada. "**3-D analytical model of axial-flux permanent magnet machine with segmented multipole-halbach array**.". *IEEE Access*, **11**:2078–2091, 2023. DOI: https://doi.org/10.1109/ACCESS.2022.3233922.